Aharonov Bohm Effect

THE
PHYSICAL REVIEW

A journal of experimental and theoretical physics established by E. L. Nichols in 1893

SECOND SERIES, VOL. 115, NO. 3 AUGUST 1, 1959

Significance of Electromagnetic Potentials in the Quantum Theory

Y. AHARONOV AND D. BOHM
H. H. Wills Physics Laboratory, University of Bristol, Bristol, England
(Received May 28, 1959; revised manuscript received June 16, 1959)

In this paper, we discuss some interesting properties of the electromagnetic potentials in the quantum domain. We shall show that, contrary to the conclusions of classical mechanics, there exist effects of potentials on charged particles, even in the region where all the fields (and therefore the forces on the particles) vanish. We shall then discuss possible experiments to test these conclusions; and, finally, we shall suggest further possible developments in the interpretation of the potentials.

assume this almost everywhere in the following discussions) we have, for the region inside the cage, $H=H_0+V(t)$ where H_0 is the Hamiltonian when the generator is not functioning, and $V(t)=e\phi(t)$. If $\psi_0(x,t)$ is a solution of the Hamiltonian H_0, then the solution for H will be

$$\psi=\psi_0 e^{-iS/\hbar}, \quad S=\int V(t)dt,$$

which follows from

$$i\hbar\frac{\partial\psi}{\partial t}=\left(i\hbar\frac{\partial\psi_0}{\partial t}+\psi_0\frac{\partial S}{\partial t}\right)e^{-iS/\hbar}=[H_0+V(t)]\psi=H\psi.$$

The new solution differs from the old one just by a phase factor and this corresponds, of course, to no change in any physical result.

EM potential for electron

Aharonov - Bohm

$$\mathcal{L} = -e\phi + \frac{e}{c}\vec{A}\cdot\vec{v} \qquad q = -e$$

long solenoid : $\vec{B} = B_0\hat{z}$

for $s > R$,

$$\vec{A} = \frac{B_0 R^2}{2s}\hat{\phi}$$

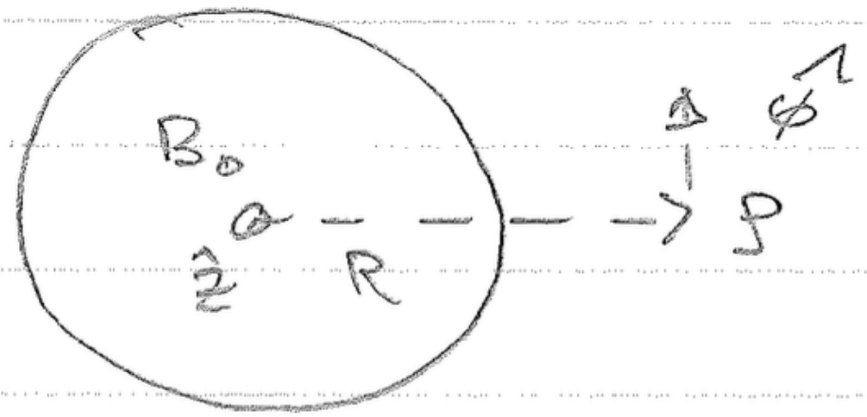

$$\oint \vec{A}\cdot d\vec{s} = \frac{B_0 R^2}{2s}(2\pi s) = B_0 \pi R^2 = \Phi_B$$

circle of constant ρ

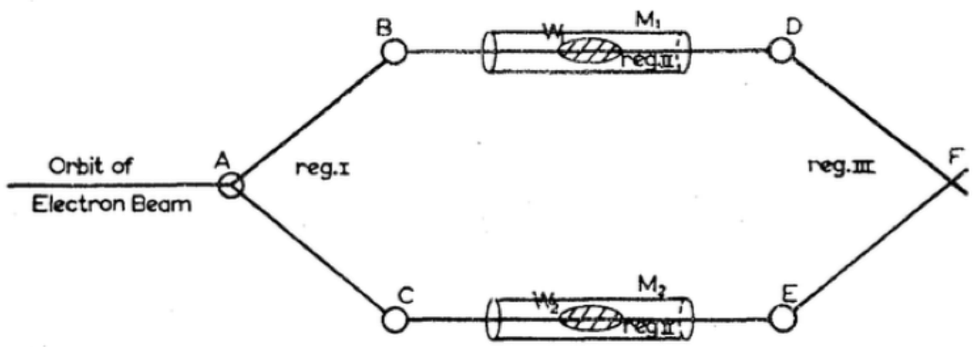

FIG. 1. Schematic experiment to demonstrate interference with time-dependent scalar potential. A, B, C, D, E: suitable devices to separate and divert beams. W_1, W_2: wave packets. M_1, M_2: cylindrical metal tubes. F: interference region.

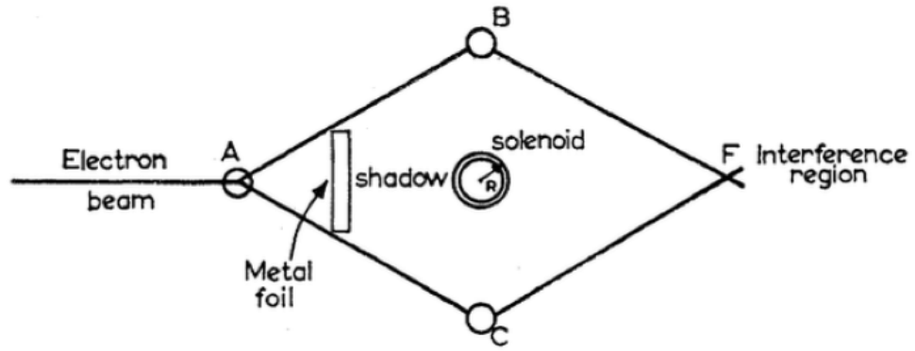

FIG. 2. Schematic experiment to demonstrate interference with time-independent vector potential.

Interference comes from electron taking **both paths**, just like Young's double slit.

one side of the solenoid and ψ_2 the beam on the opposite side. Each of these beams stays in a simply connected region. We therefore can write

$$\psi_1=\psi_1^0 e^{-iS_1/\hbar}, \quad \psi_2=\psi_2^0 e^{-iS_2/\hbar},$$

where S_1 and S_2 are equal to $(e/c)\int \mathbf{A}\cdot d\mathbf{x}$ along the paths of the first and second beams, respectively. (In Sec. 4, an exact solution for this Hamiltonian will be given, and it will confirm the above results.)

The interference between the two beams will evidently depend on the phase difference,

$$(S_1-S_2)/\hbar=(e/\hbar c)\int \mathbf{A}\cdot d\mathbf{x}=(e/\hbar c)\phi_0.$$

This effect will exist, even though there are no magnetic forces acting in the places where the electron beam passes.

$$S_{cl} = \frac{e}{c}\int_{t_1}^{t_2} \vec{A}\cdot\vec{v}\,dt = \frac{e}{c}\int_{\text{Path}} \vec{A}\cdot d\vec{s}$$

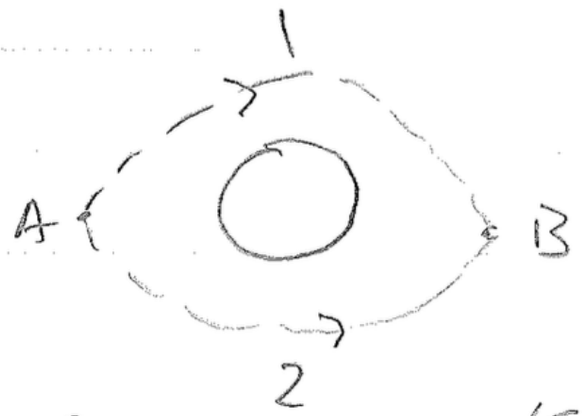

two paths interfere

$$\psi_1 + \psi_2 = e^{i\frac{S_2}{\hbar}}\left(\psi_1 e^{i(S_1-S_2)/\hbar} + \psi_2\right)$$

$$S_1 - S_2 = \frac{e}{c}\oint \vec{A}\cdot d\vec{s} = \frac{e}{c}\Phi_B \quad \text{gauge invariant}$$

1 minus 2

$$P = |\psi_1 + \psi_2|^2 = 1 + \cos\left(\frac{e\Phi_B}{\hbar c}\right)$$

P varies sinusoidally with field strength B_0.

SHIFT OF AN ELECTRON INTERFERENCE PATTERN BY ENCLOSED MAGNETIC FLUX

R. G. Chambers
H. H. Wills Physics Laboratory, University of Bristol, Bristol, England
(Received May 27, 1960)

biprism - fiber (f) metal plates (e)

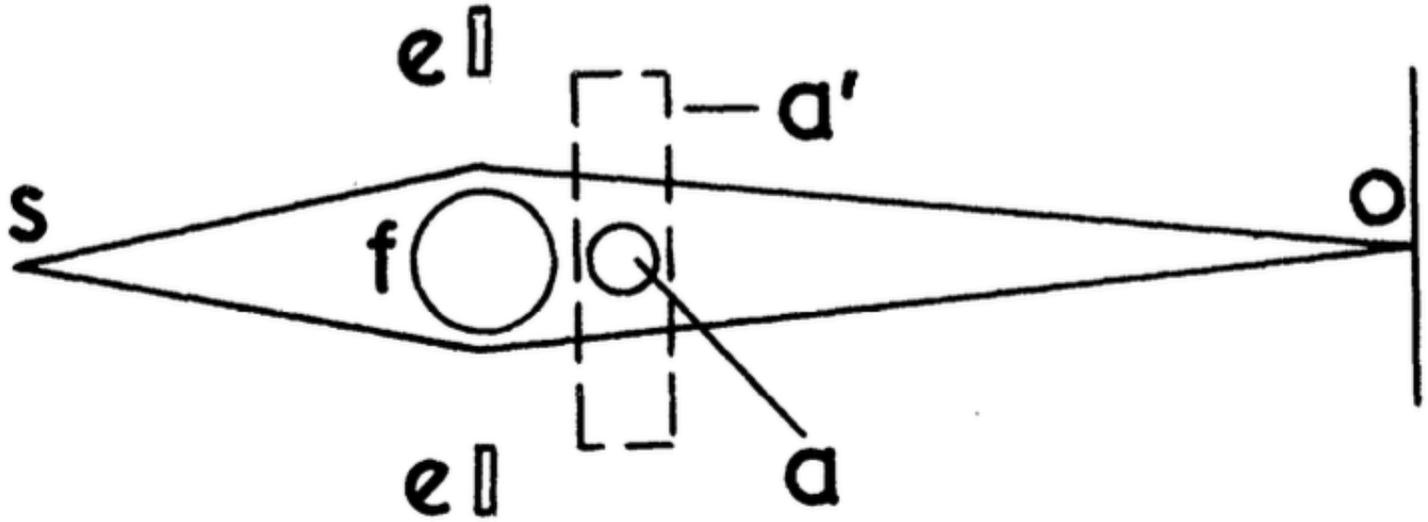

FIG. 1. Schematic diagram of interferometer, with source s, observing plane o, biprism e, f, and confined and extended field regions a and a'.

a produced by an iron whisker, about 1 μm in diameter and 0.5 mm long, placed in the shadow of the fiber f.

a' Helmholtz pair of single turns 3 mm in diameter just behind the biprism.

Field a’ as predicted the appearance of the pattern was completely unchanged.

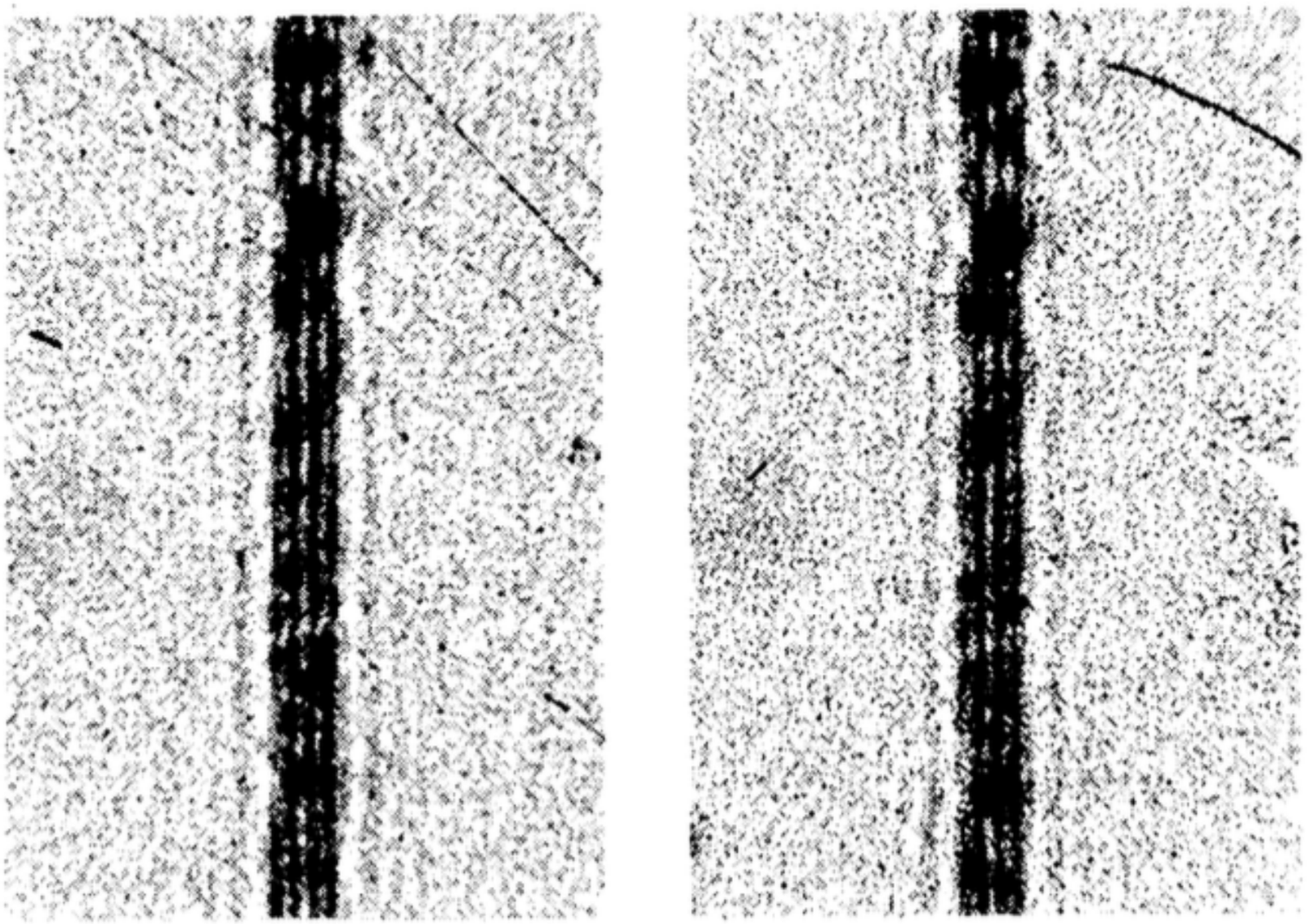

Lorentz force shift of line

(a) (b)

FIG. 2. (a) Fringe pattern due to biprism alone. (b) Pattern displaced by 2.5 fringe widths by field of type a'.

Field a (whisker) shows interference fringes

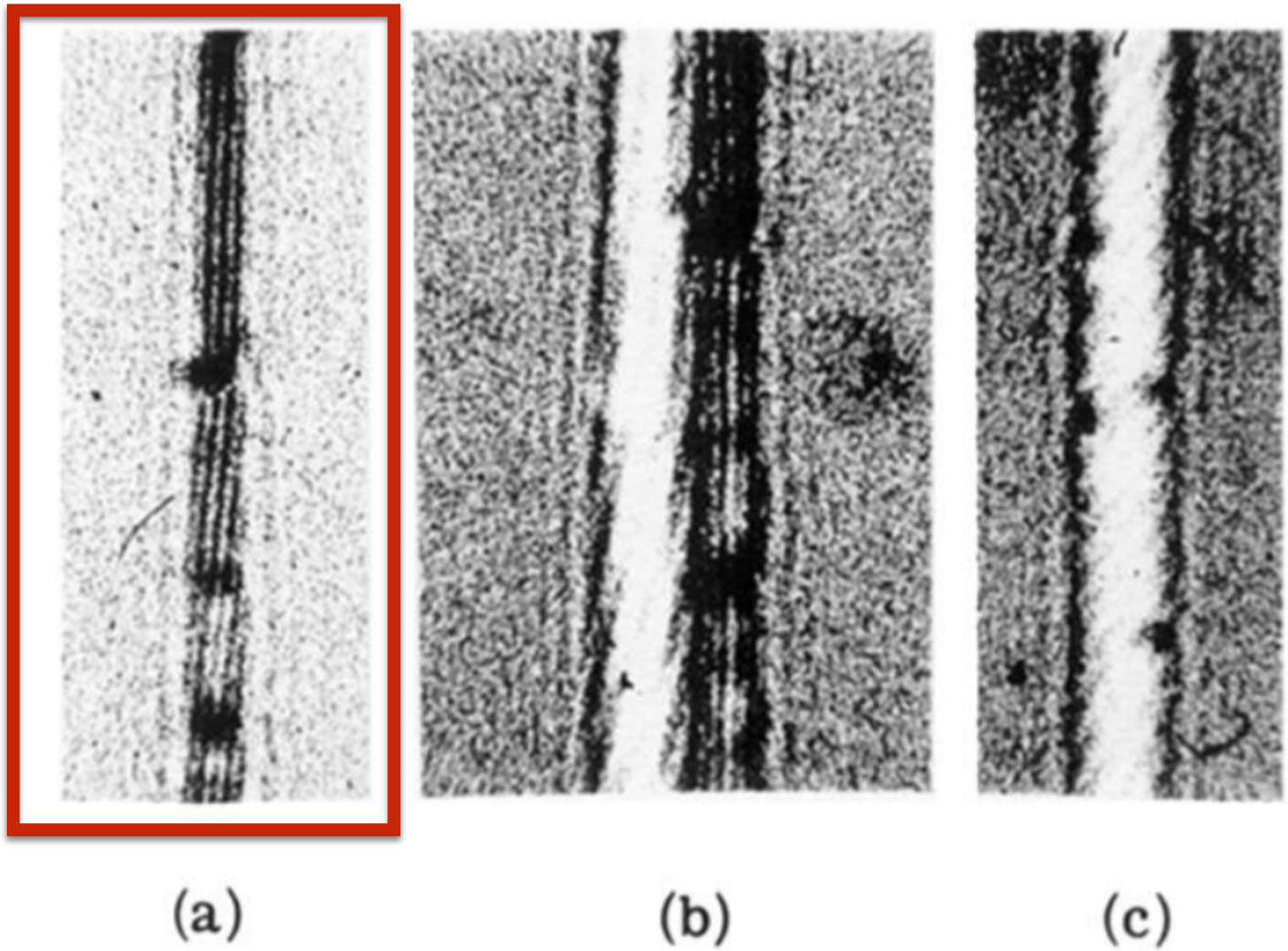

(a) (b) (c)

FIG. 3. (a) Tilted fringes produced by tapering whisker in shadow of biprism fiber. (b) Fresnel fringes in the shadow of the whisker itself, just outside shadow of fiber. (c) Same as (b), but from a different part of the whisker, and with fiber out of the field of view.

PHYSICAL REVIEW A VOLUME 34, NUMBER 2 AUGUST 1986

Experimental confirmation of Aharonov-Bohm effect using a toroidal magnetic field confined by a superconductor

Nobuyuki Osakabe, Tsuyoshi Matsuda, Takeshi Kawasaki, Junji Endo, and Akira Tonomura
Advanced Research Laboratory, Hitachi Ltd., Kokubunji, Tokyo 185, Japan

Shinichiro Yano and Hiroji Yamada
Central Research Laboratory, Hitachi Ltd., Kokubunji, Tokyo 185, Japan

(Received 21 January 1986)

The electron holography technique was employed to make a crucial test of the existence of the Aharonov-Bohm (AB) effect. The relative phase shift was measured between two electron waves passing through spaces inside and outside a tiny toroidal ferromagnet, covered completely with a superconductor layer and a Cu layer. Below the transition temperature the relative phase shift was measured to be 0 or π due to the magnetic-flux quantization in units of $h/2e$. The results directly demonstrated the existence of the AB effect even when the magnetic field was confined by the surrounding superconductor due to the Meissner effect and an electron beam was prevented from penetrating the magnet.

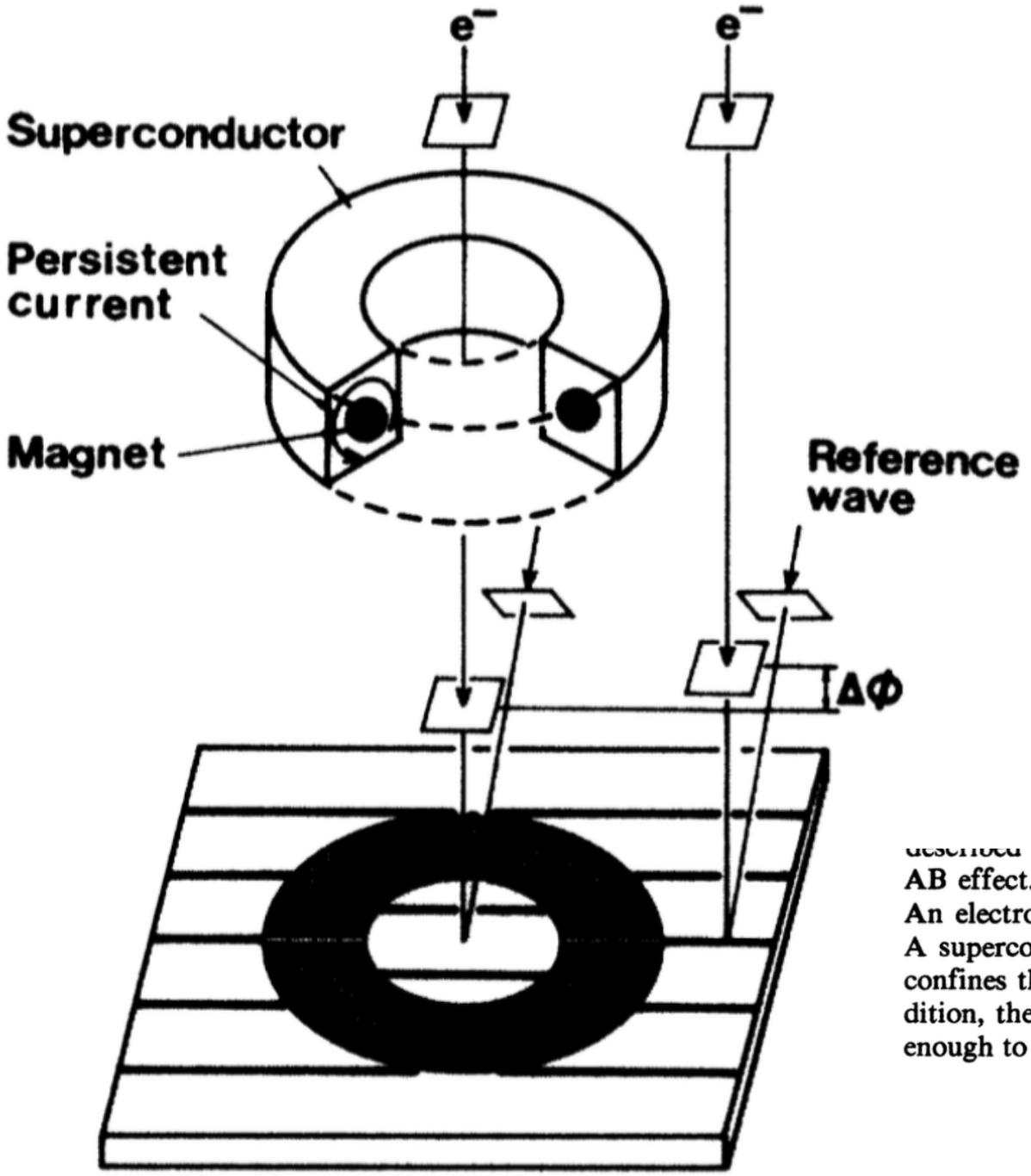

described here is designed to provide a crucial test of the AB effect.[18] The conceptual diagram is shown in Fig. 1. An electron is strictly excluded from the magnetic field: A superconductor completely covering a toroidal magnet confines the magnetic flux by the Meissner effect. In addition, the superconductor layer and a Cu layer are thick enough to prevent electron penetration.

FIG. 1. Conceptual diagram of the experiment. A Cu layer for shielding from an electron wave is not shown.

T>Tc

T<Tc

T<Tc

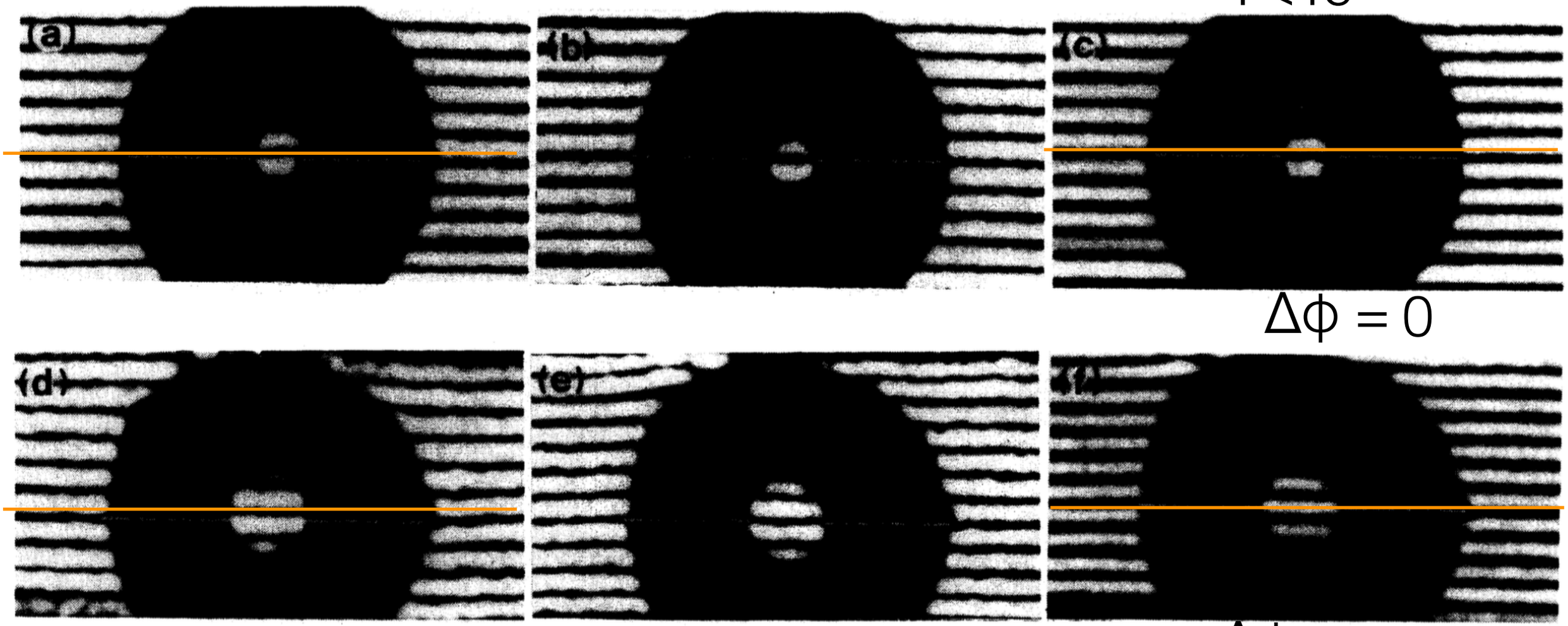

Δϕ = 0

Δϕ not quantized

Δϕ = π

2 μm

FIG. 10. Interferograms of toroids at 15 and 5 K. (a), (b), and (c): magnetic flux is quantized in $n(h/2e)$ (n is even) below T_c. The toroid is $R1$ (see Table I); (d), (e), and (f): magnetic flux is quantized in $n(h/2e)$ (n is odd) below T_c. The toroid is $R2$. (a) and (d), $T=15$ K (phase amplification, $\times 2$). (b) and (e), $T=5$ K (phase amplification, $\times 2$). (c) and (f), $T=5$ K (phase amplification, $\times 1$).

February 1998 letters to nature

Dephasing in electron interference by a 'which-path' detector

E. Buks, R. Schuster, M. Heiblum, D. Mahalu & V. Umansky

Braun Center for Submicron Research, Department of Condensed Matter Physics, Weizmann Institute of Science, Rehovot 76100, Israel

Wave–particle duality, as manifest in the two-slit experiment, provides perhaps the most vivid illustration of Bohr's complementarity principle: wave-like behaviour (interference) occurs only when the different possible paths a particle can take are indistinguishable, even in principle[1]. The introduction of a which-path (*welcher Weg*) detector for determining the actual path taken by the particle inevitably involved coupling the particle to a measuring environment, which in turn results in dephasing (suppression of interference). In other words, simultaneous observations of wave and particle behaviour is prohibited. Such a manifestation of the complementarity principle was demonstrated recently using a pair of correlated photons, with measurement of one photon being used to determine the path taken by the other and so prevent single-photon interference[2]. Here we report the dephasing effects of a which-path detector on electrons traversing a double-path interferometer. We find that by varying the sensitivity of the detector we can affect the visibility of the oscillatory interference signal, thereby verifying the complementarity principle for fermions.

In our experiment we used a double-path electronic interferometer[5], fabricated within the plane of a high-mobility two-dimensional electron gas. The two paths are defined by two slits electrons can pass through, with one slit in the form of a coherent quantum dot (QD)[5,6]. The QD is a trap that captures electrons for a relatively long time, like a resonant delay line, thus allowing the electrons to be detected more easily. Near the QD, but electrically separated from it, a quantum point contact (QPC) is fabricated, serving as a which-path detector. The QPC is a short conducting segment with width comparable to the electron wavelength, allowing only a small number of modes to pass. It is expected that an electron passing the QD-slit will interact with the nearby QPC-detector (both systems are thus 'entangled'[7]) and modify the conductance of the QPC[8]. This detection process leads to dephasing, that is, to a suppression of the double-path Aharanov–Bohm interference.

quantum point contact (QPC) measures e- path with some probability

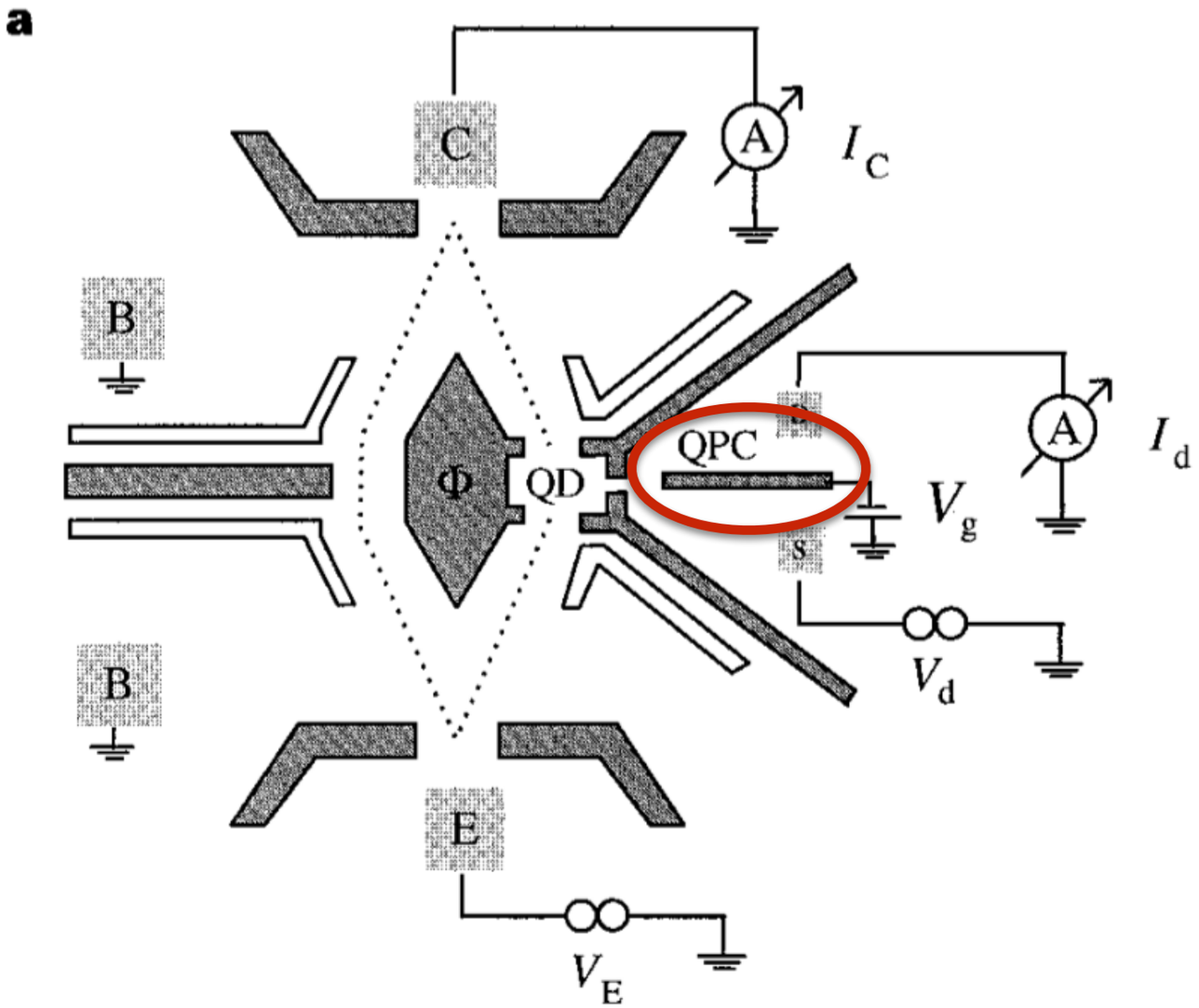

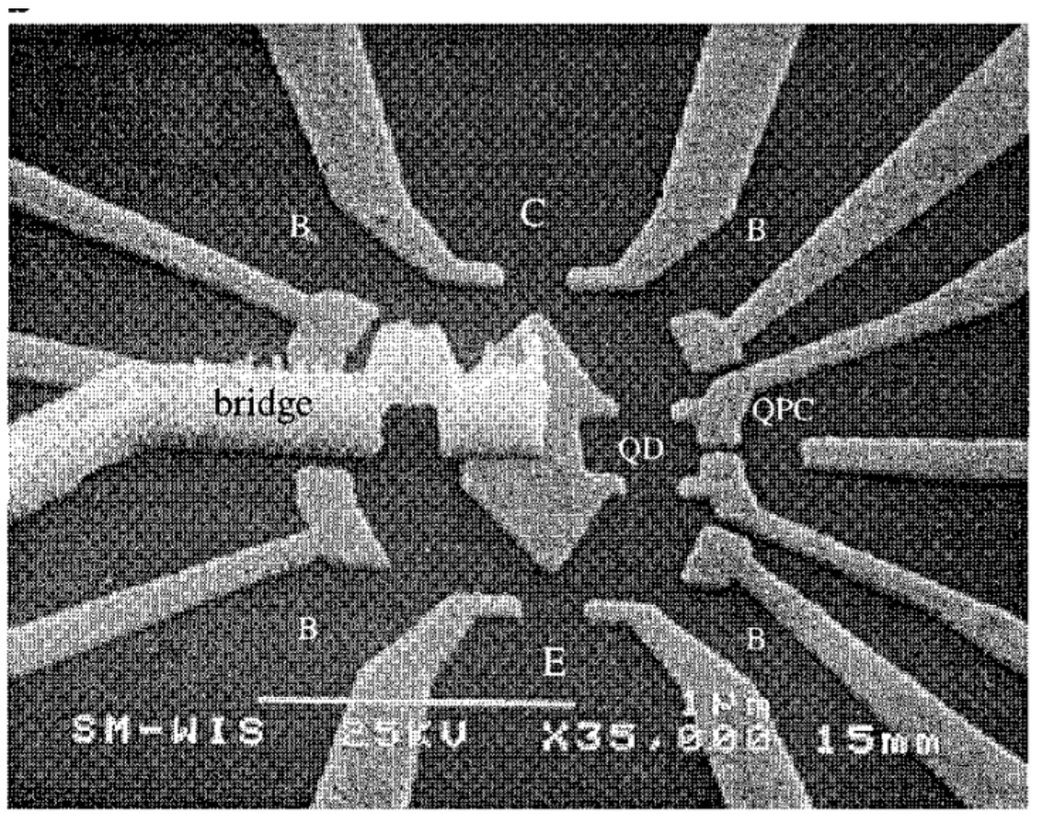

Aharonov-Bohm effect

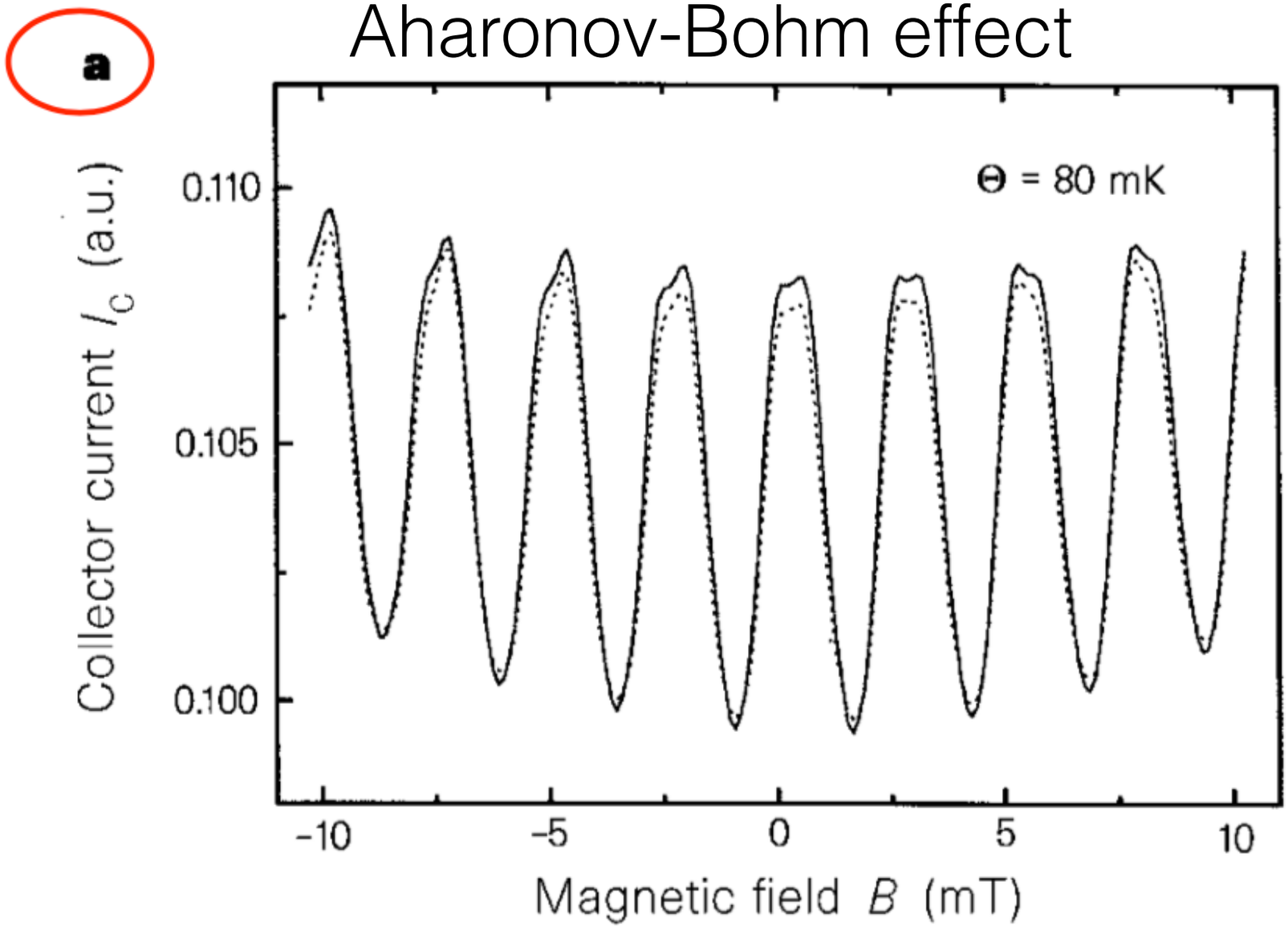

Fig. 1a; longer paths, resulting from multiple reflections from walls, are much less probable. A phase difference between the two direct paths, $\Delta\alpha = 2\pi\Phi/\Phi_0$, is induced via the Ahoronov–Bohm effect (for a review see ref. 10). Here Φ is the magnetic flux threaded through the area, A, enclosed by these two paths and $\Phi_0 = h/e$ is the flux quantum. Consequently, the collector current oscillates as a function of magnetic field B with a period $\Delta B = \Phi_0/A = 2.6\,\mathrm{mT}$, corresponding to a phase difference between the two paths equal to 2π, as seen in Fig. 2a.

How certain is our which-path detection? An electron entering the QD-slit changes the transmission probability of the QPC-detector by ΔT_d. The rate at which particles probe the detector at zero temperature is $2eV_d/h$, where V_d is the voltage across the detector. Thus, the number of particles probing the detector

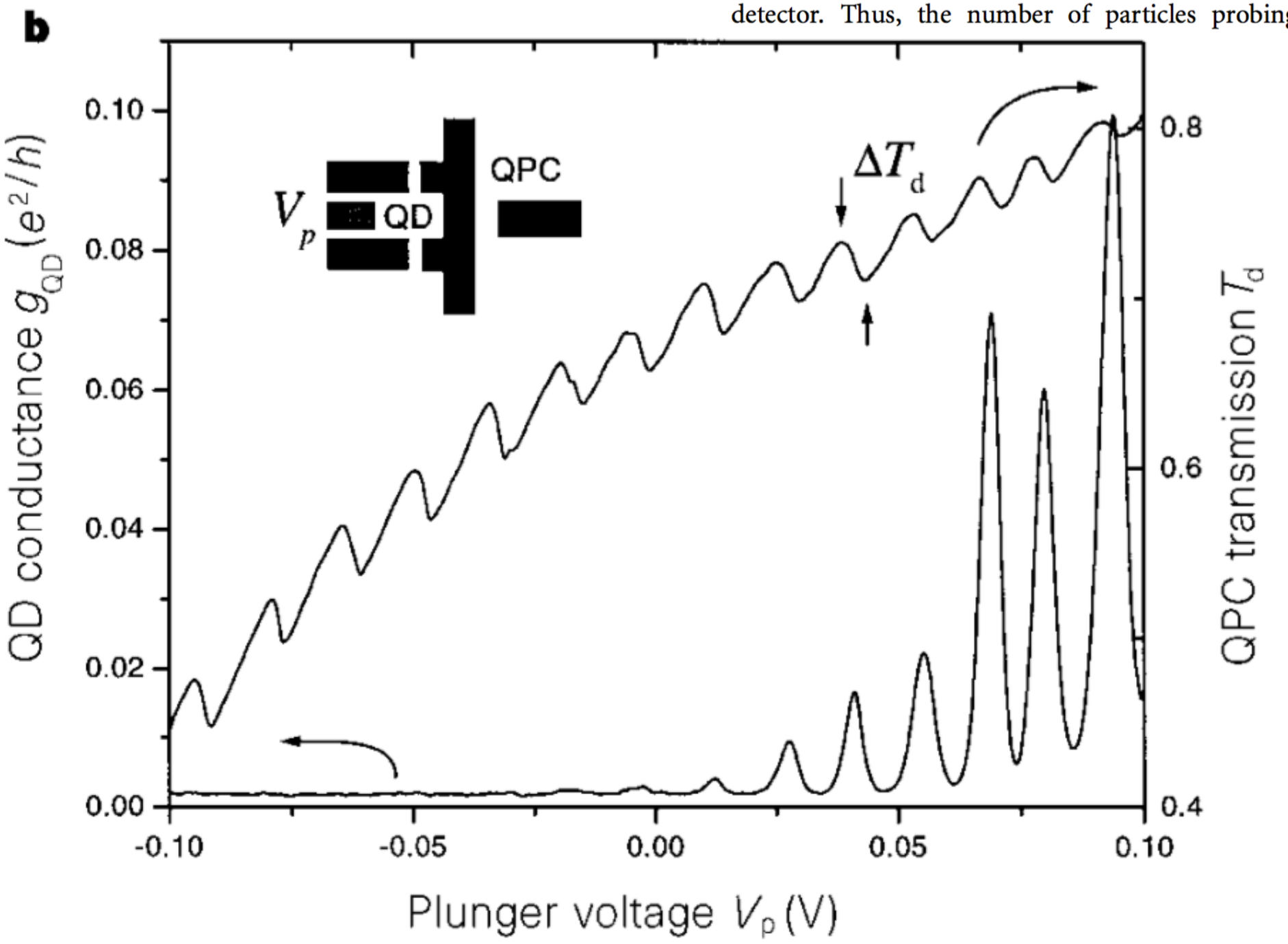

with $V_d = 100\,\mu$eV. (a.u., arbituary units.) **b**, The conductance of the QD, g_{QD}, and the transmission of the QPC nearby, T_d, as a function of the plunger gate voltage, V_p. The inset shows schematically the coupled structures. **c**, The induced

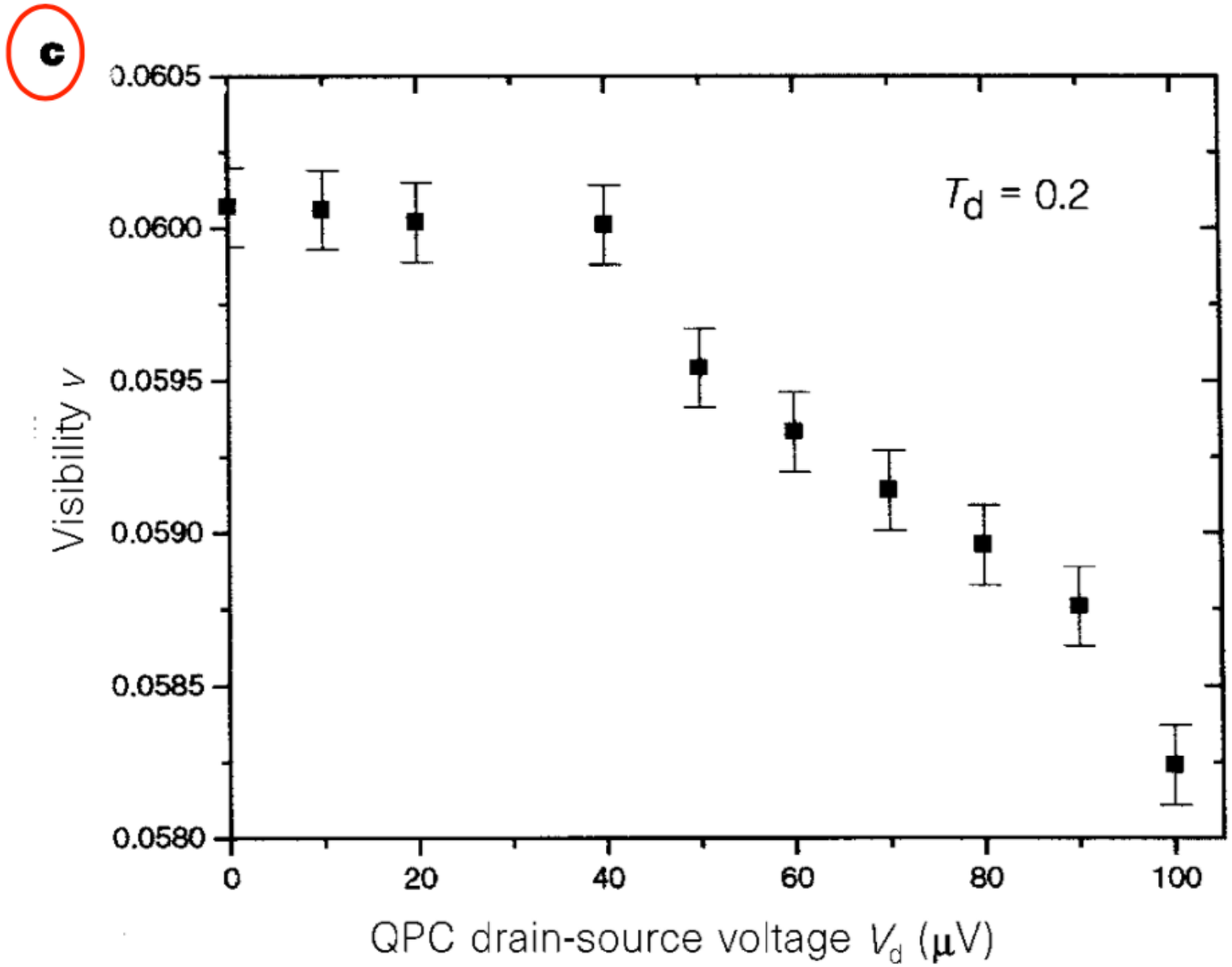

remaining oscillatory component squared leads to the peak-to-valley value. Last, the visibility is found by dividing by the average value of I_C. Error bars indicate the fluctuations in visibility due to fluctuations of device's properties (instrumental noise is negligibly small). **c**, The visibility of the AB conductance oscillations as a function of V_d for a fixed $T_d = 0.2$. The behaviour is linear for $eV_d > k_B\Theta$ with saturation for low V_d.

$=7\mu eV$

interference decreases with determination of which path